QUARTERLY JOURNAL
OF THE
ROYAL METEOROLOGICAL SOCIETY

Vol. 127 JULY 2001 Part B No. 576

Q. J. R. Meteorol. Soc. (2001), **127**, pp. 1869–1891

Ocean–atmosphere–land feedbacks in an idealized monsoon

By C. CHOU, J. D. NEELIN* and H. SU
University of California, Los Angeles, USA

(Received 30 March 2000; revised 27 February 2001)

SUMMARY

An intermediate-complexity atmospheric model coupled with a simple land-surface model and a mixed-layer ocean model is used to investigate the processes involved in an idealized monsoon occurring on a single rectangular continent. Idealized divergences of ocean heat transports are specified as an annual average 'Q-flux'. In this simple coupled configuration, the mechanisms that affect land–ocean contrast and, in turn, the seasonal movement of the continental convergence zones are examined. These include soil-moisture feedbacks; cooling of tropical oceans by ocean transport; ventilation, defined as the import into continental regions of low moist static-energy air from ocean regions where heat storage opposes summer warming; and the 'interactive Rodwell–Hoskins mechanism', in which Rossby-wave-induced subsidence to the west of monsoon heating interacts with the convection zone. The fixed ocean transports have a substantial impact on the continental convection. If Q-flux is set to zero, subtropical subsidence and ventilation tend to substantially limit the poleward movement of summer monsoon rainfall. When land hydrology feedbacks are active, the drying of subtropical continents disfavours continental convection even in the tropics. When ocean transports are included, tropical oceans are slightly disfavoured as regions for producing convection which, by contrast, favours continental convection. The monsoon circulation then produces moisture transport from the ocean regions that allows substantial progression of convection into the subtropics over the eastern portion of the continent. The western portion of the continent tends to have a dry region of characteristic shape. This east–west asymmetry is partly due to the interactive Rodwell–Hoskins mechanism. The ventilation is of at least equal importance in producing east–west asymmetry and is the single most important process in limiting the poleward extent of the continental convection zone.

KEYWORDS: Convergence zone Monsoon Ocean–atmosphere–land feedback Ocean heat transport Tropical convection Soil moisture

1. INTRODUCTION

The monsoon is a complicated climate phenomenon involving interactions between ocean, atmosphere and land. Land processes, such as soil moisture, evapotranspiration, surface albedo (Xue and Shukla 1993; Meehl 1994; Lofgren 1995; Yang and Lau 1998) and topography (Flohn 1957; Murakami 1987; Yanai *et al.* 1992; Yanai and Li 1994), affect the magnitude and position of the monsoon. The ocean, through sea surface temperature (SST) variation, plays a role in determining monsoon circulation (Nobre and Shukla 1996; Trenberth *et al.* 1998). The monsoon is a global-scale phenomenon and is interactive with other large-scale circulations. For instance, the Asian–Australian monsoon circulation is linked to the ascending branch of the Walker circulation (Webster 1994), while the descending branch of the Walker circulation contributes to desertification in regions such as northern Africa. Rodwell and Hoskins (1996) proposed a monsoon–desert mechanism to explain an interaction between the Asian monsoon regions and the Sahara/Mediterranean and Aral Sea regions. In the northern summer, a

* Corresponding author: Department of Atmospheric Sciences, University of California, Los Angeles, Los Angeles, CA 90095-1565, USA. e-mail: neelin@atmos.ucla.edu

remote diabatic heating of the monsoon in southern Asia provides Rossby-wave-related subsidence for desertification in northern Africa. Monsoon circulation also has an interannual variability which is interactive with other global phenomena, such as the El Niño Southern Oscillation (ENSO) (Ju and Slingo 1995; Webster *et al.* 1998; Webster and Yang 1992) and the tropospheric biennial oscillation (TBO) (Tian and Yasunari 1992; Shen and Lau 1995).

Simplifications made in a number of studies clarify the roles of some processes occurring in the monsoon circulation. For example, Cook and Gnanadesikan (1991) simplified land hydrology using idealized boundary conditions. In an atmospheric general-circulation model (AGCM) with fixed SST, they studied the effects of soil moisture on the tropical circulation. They concluded that the intertropical convergence zone (ITCZ) moves further poleward in the summer hemisphere and is enhanced near the coast for a saturated continent. Changes in low-level moisture convergence related to tropical circulation are associated with the poleward shifting of the continental ITCZ. Dirmeyer (1998) used an AGCM coupled with the simple biosphere model (SiB) (Sellers *et al.* 1986) to study the role of land–ocean geometry in monsoons. He found that latitudinal position of the continent had a substantial impact on the seasonal variation of continental precipitation and on the summer monsoon circulation. A zonal asymmetry was seen in the continental rainfall distribution, with enhanced rainfall tending to occur on the eastern side of the continent and large dry regions toward the western side. He also noted the importance of what he termed 'the battle for tropical moisture supply', between continent and ocean. Srinivasan *et al.* (1993) used a simple ocean–atmosphere model and a ground-hydrology model to discuss the meridional propagation of the monsoon convective zone. Shukla and Fennessy (1994) performed experiments with fixed SST and fixed solar forcing to examine the importance of solar forcing on land and the annual cycle of SST. Webster and Chou (1980a, 1980b) used a zonally symmetric ocean–atmosphere–land climate model to simulate northward propagation of a monsoon system.

Nonetheless, many aspects associated with monsoon mechanisms are poorly understood. The Atmospheric Model Intercomparison Project (AMIP) from the Tropical Ocean Global Atmosphere (TOGA) Monsoon Numerical Experimentation Group (MONEG) evaluates the ability of 32 AGCMs in simulating precipitation over the Indian subcontinent, the African Sahel, and the Nordeste region of Brazil (Sperber and Palmer 1996). With identically specified SST, the results show strong variation of precipitation over India and the Sahel from model to model. These suggest that some processes associated with monsoon mechanisms have not been simulated adequately in some or all of the AGCMs. In coupled systems simulating monsoon climate becomes more challenging. Many coupled general-circulation models (CGCMs) have inaccurately simulated monsoon climate (Meehl 1989; Latif *et al.* 1994). The complexity of the CGCMs renders it difficult to identify causes for these problems. We use a prototype coupled system which may help to diagnose and understand the GCM results. This simple coupled system includes an atmospheric model and a land-surface model with intermediate complexity (Neelin and Zeng 2000; Zeng *et al.* 2000, ZNC hereafter), as well as a simple mixed-layer ocean model. The mixed-layer ocean model uses a so-called 'Q-flux' to mimic divergence of ocean heat transport (Hansen *et al.* 1988, 1997). Although simple, this model allows us to examine what we believe is an overlooked aspect of the monsoon problem: the role of ocean heat transport in producing land–ocean contrast.

Many monsoon studies focus on local aspects, such as the effects of topography and the geometry of the continent. However, the monsoon can also be viewed in a more general aspect: the monsoon is the movement of a planetary-scale convergence

zone. We de-emphasize the flow pattern of the monsoon circulation because it is not universal for all monsoons, e.g. the North American monsoon does not have cross-equatorial flow. Land–ocean heating contrast plays an important role in creating monsoon circulation (Webster 1987; Young 1987). To simulate this land–ocean contrast, an idealized rectangular geometry of the continent with a homogeneous land surface and no topography is introduced. In this study, we address several general questions regarding monsoon circulation, such as the relative roles of soil moisture and ocean heat transport in producing land–ocean contrast. In the summer hemisphere, land tends to heat up faster than ocean. Based on a thermodynamic argument, the convergence zone should follow the maximum heat input into the atmosphere if there is enough moisture supply. However, the monsoon does not simply follow the solar maximum heating which extends poleward during the summer. At midlatitudes, dominant westerly winds tend to advect air with low moist static energy from the ocean, where ocean heat storage keeps summer SST cool, into the continent. We term this the 'ventilation effect', and it tends to balance the heating by solar radiation. What sets the poleward extension of the monsoon: soil-moisture feedbacks or the ventilation effect?

A detailed description of the coupled model system is discussed in section 2. In the equinox case described in section 3, we examine the effect of soil moisture and ocean transport. In section 4, we discuss seasonal variation of continental convection and ventilation by cross-continental flow. Causes for east–west asymmetry of continental convection are analysed in section 5. The impact of a wider continent is seen in section 6, followed by conclusions.

2. MODEL DESCRIPTION

The atmospheric model used in this study is a quasi-equilibrium tropical circulation model (QTCM) developed by Neelin and Zeng (2000) and ZNC. It is a class of model for the tropical circulation that exploits the constraints placed on the flow by convective parametrizations with quasi-equilibrium (QE) thermodynamic closures. For the QE closure, a version of the Betts and Miller (1986, 1993) deep-convection scheme is used. Analytical solutions are derived by Neelin and Yu (1994) and Yu and Neelin (1994). Neelin (1997) summarizes a method using the analytical solutions as leading basis functions for a Galerkin expansion in the vertical. We refer to the model used here, which has a single vertical structure of deep convection for temperature and humidity, as QTCM1. Because the basis functions are tailored to vertical structures associated with convective regions, these regions are expected to be well represented in QTCM1. Far from deep convective regions, QTCM1 is a highly truncated Galerkin representation equivalent to a two-layer model. With its intermediate complexity, between a full GCM and simpler models, this model is easier to analyse, is numerically faster than a GCM, and has more physical processes than simpler models.

To accompany the representation of dynamics in this model, a cloud-radiation package is employed (Chou and Neelin 1996; Chou 1997; Chou and Neelin 1999) that represents the main cloud radiative processes at an intermediate level of complexity. This includes a long-wave radiation parametrization (Chou and Neelin 1996) derived from GCM parametrizations, a simple linear calculation of short-wave radiation based on Fu and Liou (1993), and an empirical parametrization for deep and cirrocumulus/cirrostratus cloud fraction (Chou and Neelin 1999). This physical parametrization package can give near GCM-like accuracy in the determination of radiative flux exchange at the surface under suitable circumstances. Caveats for the application here include lack of prognostic low and middle clouds.

Similar in structure to the physical parametrization package, the land-surface model (ZNC) with intermediate complexity includes the essentials of complex land-surface models, such as the biophysical control on evapotranspiration and surface hydrology, but retains computational and diagnostic simplicity. This model is designed to capture land-surface effects for climate simulation at time-scales longer than a day. This model uses a single land-surface layer for both energy and water budgets. Since the heat capacity of land is small, the net surface heat flux is essentially close to zero on a time-scale longer than a day. Surface-heat flux is balanced by solar radiation, long-wave radiation, evaporation and sensible-heat flux. The prognostic equation for soil moisture includes precipitation, evaporation, surface run-off and ground run-off. Surface run-off increases as the soil moisture reaches a saturation value that depends on surface type.

To study the interaction between the atmosphere and land, a fixed SST is commonly assumed in climate models in order to simplify the simulation. To avoid any artificial effects induced by the contrast of fixed SST boundary conditions and interactive land surfaces, an ocean surface layer with active thermodynamics is included in the simulations presented here. Instead of coupling a complicated ocean general-circulation model, a slab mixed-layer ocean model with a fixed mixed-layer depth of 50 metres is used. By specifying Q-flux, which crudely simulates divergence of ocean transport (Hansen *et al.* 1988, 1997), SST can be determined by the energy balance between surface radiative flux, latent-heat flux, sensible-heat flux and Q-flux. The Q-flux can be obtained from observations or ocean model results (Miller *et al.* 1983; Russell *et al.* 1985; Keith 1995; Doney *et al.* 1998). In general, the Q-flux varies from ocean to ocean as well as from season to season. In this study, we specify Q-flux purely as a function of latitude and we exclude seasonal variation:

$$\text{Q-flux} = \cos(\varphi \times 3.5) \times Q_{\max} \tag{1}$$

with the maximum value ($Q_{\max}$) at the equator, and latitude φ in radians. The magnitude of Q-flux is roughly estimated to match the zonal average from the observed annual mean.

To simplify the effect of the land geometry in order to understand ocean–atmosphere–land interaction, an idealized rectangular land surface is specified here. The standard width of the land is similar to the width of Africa or South America (45° in longitude). A continent that is symmetric about the equator is chosen so that it is clear that asymmetry about the equator in the summer monsoon is associated purely with seasonal effects. Simulations have also been conducted with a rectangular continent north of 8°N and ocean to the south. These yield similar results for the large-scale processes considered and are, therefore, not shown. Figures and discussion focus on the northern-hemisphere summer, but all would apply as well to the southern-summer case (asymmetries due to perihelion are small). There is no topography over land, and only one surface type is used for each experiment. To ensure that land–ocean contrast is due to primarily dynamical factors (transport and storage), and is not induced by difference of albedo over ocean and land, surface albedo is set to be the same constant over both land and ocean. This permits other processes to be seen more clearly. The model predicts only deep cloud and cirrostratus/cirrocumulus, which is much less than total cloud cover, and no snow cover is predicted over land. In order to have the globally averaged albedo for the model close to the observed albedo, 0.3 is used for the model surface albedo. Simulations with realistic continental configurations, albedo, etc. are considered in other work (Chou and Neelin 2001).

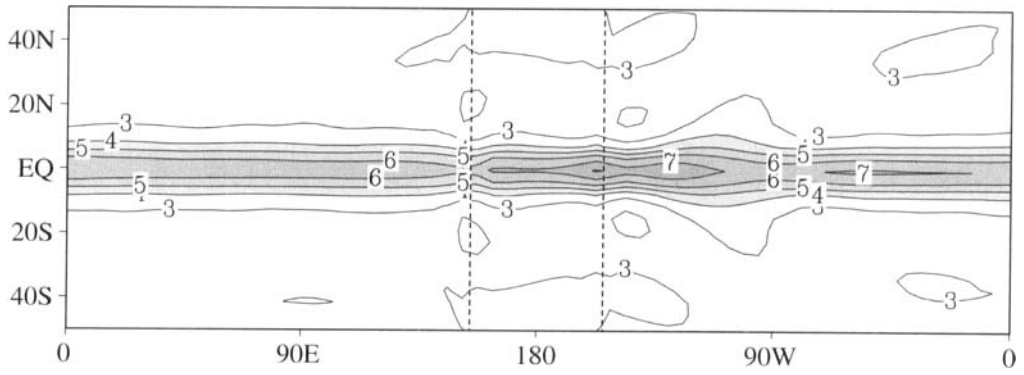

Figure 1. Precipitation (mm day^{-1}) for an experiment with zero Q-flux, equinox conditions, and saturated soil moisture. Only part of the model latitudinal domain (60°S–60°N) is shown. The continent is indicated by dashed lines.

3. Impacts of soil moisture and ocean transport in an equinox experiment

(a) *Soil moisture*

We first focus on the effect of soil moisture, without the contribution from ocean transport, so zero Q-flux is specified. Two experiments are performed here: saturated, and interactive soil moisture. In the saturated soil-moisture experiment, soil moisture is forced to maintain saturation, but surface temperature is calculated from the surface heat flux budget. For the interactive soil-moisture experiment, land hydrology is active, so land is not only balanced in the heat flux but also in the water budget. For simplicity, a forest surface type is specified.

Figure 1 shows precipitation averaged over 10 years for the saturated-soil-moisture case. The ITCZ is at the equator and patterns of precipitation over land are similar to precipitation over ocean. Differences in surface temperature between the continent and the ocean are small. In this experiment, the continent acts like a swamp, and can supply water indefinitely. Over the continent, averaged over a time-scale longer than several days, the net surface heat flux is close to zero because of the small heat capacity of land. With zero Q-flux and averaged over a much longer time-scale (more than a year; 10-year averages shown here), the net heat flux over the ocean is also zero. Therefore, the only differences between the continent and the ocean are heat capacity and surface roughness. For equinox conditions and a long time average, the difference in heat capacity between continent and ocean is less important. Although the nonlinear response to transient variations can produce some effects, these appear to be secondary. While surface roughness affects surface wind stress and surface heat flux, through sensible heat and evaporation, for large-scale features these effects likewise appear to be secondary.

Figure 2 shows precipitation for the interactive soil-moisture experiment. Precipitation over the subtropical continent decreases significantly. When land hydrology is interactive, soil moisture cannot maintain the saturated level. In the subtropical subsidence regions (the descending branch of the Hadley cell), the low precipitation leads to low values of soil moisture. Evaporation from land surface decreases, and surface temperature increases in order to balance surface heat flux. Sensible heat and long-wave radiation become more important processes in exchanging heat flux between the land and the atmosphere. With less moisture in the atmosphere, the convective available potential energy (CAPE) decreases, so convection becomes less frequent. This results

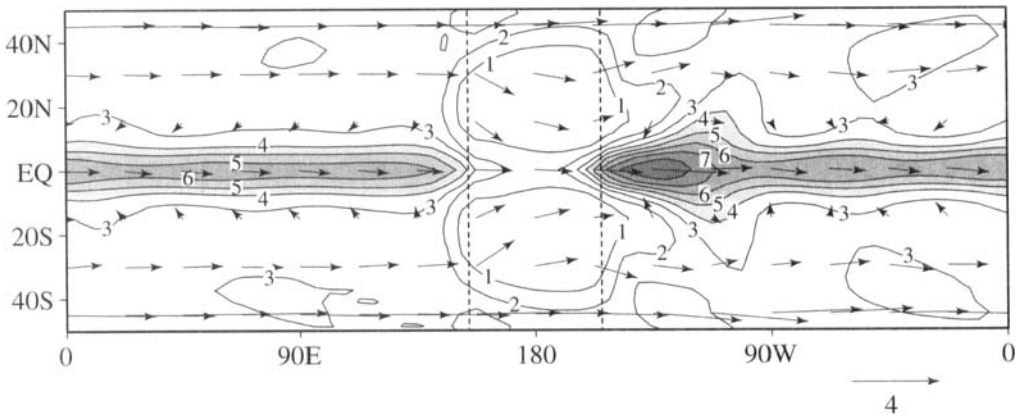

Figure 2. As in Fig. 1, except for interactive soil moisture. The vectors are 850 mb winds (m s^{-1}, shown at 1/4 of the grid points).

in less precipitation which further intensifies the dryness of the subtropical (and also midlatitude) continent.

An increase of surface temperature over the subtropical continent induces a subtropical circulation. The low-level wind (Fig. 2) over the continent is a westerly anomaly at lower latitudes and an easterly anomaly at higher latitudes. It is opposed to the mean zonal wind which transports moisture to the continent from the ocean. Due to the weakening of the horizontal transport of moisture, land precipitation decreases near the equatorial area, but on the eastern coast and the eastern coastal waters, precipitation increases. Less convection over the subtropical continent results in less cloud reflection, so more solar radiation reaches the surface. This further increases surface temperature over the continent. The subtropical circulation becomes stronger and the continent becomes drier. Where the continent is wider, moisture decreases, especially at the centre of the continent. It is evident that the subtropical circulation weakens the moisture transport from the ocean to the continent. As subtropical circulation increases, drier air from the subtropics converges meridionally into the continental ITCZ. Thus, the continental ITCZ is weakened considerably (Fig. 2). This is quite different from what one expects from observations, so there must be some countervailing process. It serves to underline that if interactive land hydrology were the main player in determining land–ocean contrasts, the continents would tend to be disfavoured. We next examine how this changes when ocean transports are included.

(*b*) *Ocean transport*

In the experiments shown in Fig. 1 and Fig. 2, zero Q-flux is assumed, i.e. ocean transports of heat are neglected. We now consider the very simple case of zonally symmetric ocean transports of the form given by Eq. (1), where Q_{max} measures the strength of the divergence of the heat transport. Figure 3 shows precipitation with interactive soil moisture for $Q_{max} = 20$ W m^{-2}, which is similar to the zonal average of a smoothed observed net surface heat flux. Stronger precipitation occurs over the continent near the equator, and relatively weak precipitation is found over the ocean in the tropics. In the tropics, the ocean acts as an energy sink for the atmosphere (positive Q-flux) because the heat is transported to higher latitudes within the ocean. Over land, on time-scales much longer than a day (here a month), net heat flux is near zero. Based on the difference of net surface heat flux over ocean and over land, there is less net heat

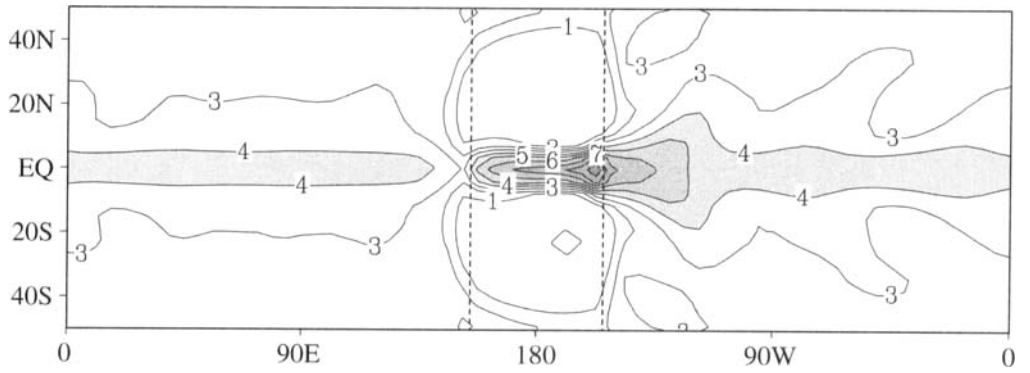

Figure 3. Precipitation (mm day^{-1}) for an experiment with maximum Q-flux, $Q_{max} = 20$ W m^{-2}, equinox conditions, and interactive soil moisture.

flux into an air column (F^{net}) over the ocean than over the continent. The continent becomes favoured for deep convection relative to the ocean. Strong precipitation is also found further inland on the tropical continent, because large-scale convergence, induced by stronger convection, imports moisture from the ocean into the centre of the tropical continent. Overall, a realistic magnitude of zonally averaged heat transport is able to overcome the soil-moisture effect of the previous section so far as tropical continental convergence zones are concerned.

Compared with Fig. 2 for the ocean area, Fig. 3 shows that precipitation over the tropical ocean decreases. Besides the impact on large-scale convergence, ocean heat transport can change the distribution of SST. When the ocean transports heat in the tropics to higher latitudes, SST decreases in the tropics and increases at higher latitudes. The north–south gradient of SST is reduced. Since SST affects atmospheric temperature, the mean zonal wind is weakened, as is the Hadley circulation.

In reality, ocean transport varies from ocean to ocean and from season to season, so the effect is likely to be more complex than the idealized experiments predict. This simple case serves to underline the role of the annually averaged heat transport in producing land–ocean contrast. This effect remains important even in the seasonal case discussed below.

4. Seasonal climatology

(a) *Impact of soil moisture and ocean transport*

With solar radiation varying seasonally, the heat-capacity difference between ocean and land becomes critical. For a mixed layer at a depth of 50 metres, it takes several years to reach thermodynamic equilibrium on large scales, so heat storage is important on seasonal time-scales. Figure 4(a) shows precipitation in June for zero Q-flux with saturated soil moisture. The month of June is chosen here to coincide with maximum insolation in the northern hemisphere during summer. Results for July are similar. In Fig. 4(a), the monsoon over the continental region (continental convection zone) is slightly north compared with the convection zones over the ocean. There is an asymmetry in the precipitation pattern over the continental region, with the precipitation concentrated over the east coast. It is interesting to note that the land–sea contrast in heat capacity does not produce as huge a contrast in land versus ocean convection zones as one might expect—the reasons for this are discussed in section 4(b).

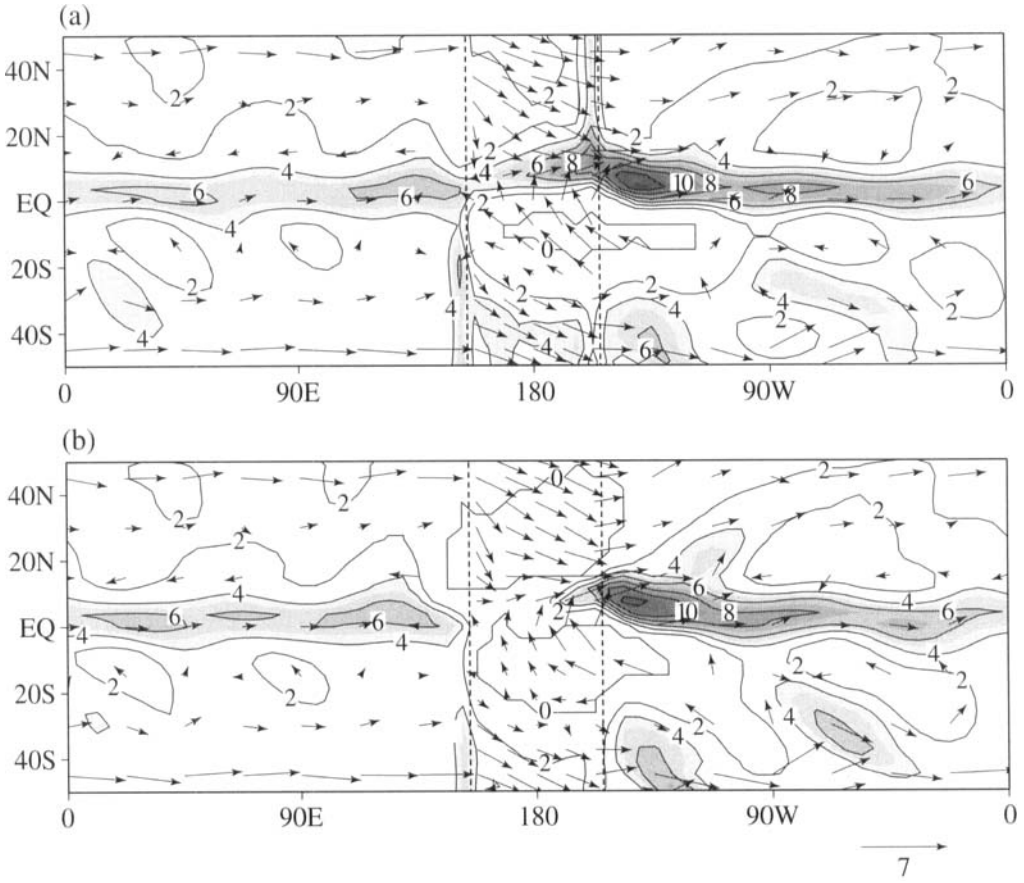

Figure 4. Precipitation (mm day^{-1}) in June for (a) saturated soil moisture with no Q-flux, (b) interactive soil moisture with no Q-flux. The vectors are 850 mb winds (m s^{-1}, shown at only 1/4 of the grid points over oceans).

When the land hydrology is active (Fig. 4(b)), soil moisture becomes important in determining precipitation over the continental region for this zero Q-flux case. Compared with the perpetual-equinox case (Fig. 2), many of the same effects occur despite the presence of the seasonal cycle. In the dry season, subtropical subsidence reduces soil moisture. During the summer, insolation favours movement of the convection zone as in Fig. 4(a), but low soil moisture leads to lower evapotranspiration, so it is harder to reach values of low-level moisture that would permit convection. The continental region is thus disfavoured relative to the ocean, resulting in large regions with no convection and continental subsidence even in summer. The land hydrology mechanism can thus limit the poleward extent of the convergence zone. Xie and Saiki (1999) note in their model that half of the continental precipitation is contributed by local evaporation from land. The tropical continental convection zone is also affected by the import of low moisture (850 mb winds in Figs. 4(a) and (b)), as occurred in the equinox case.

The soil-moisture feedback does, however, depend on the large-scale environment set by land–sea differences. If other circulation factors permit, soil moisture gained from precipitation can keep atmospheric moisture high, leading to more precipitation. For example, in Xie and Saiki's (1999) perpetual runs, the model monsoon penetrates deep inland because of high soil moisture. Ocean heat transport, even if not seasonally

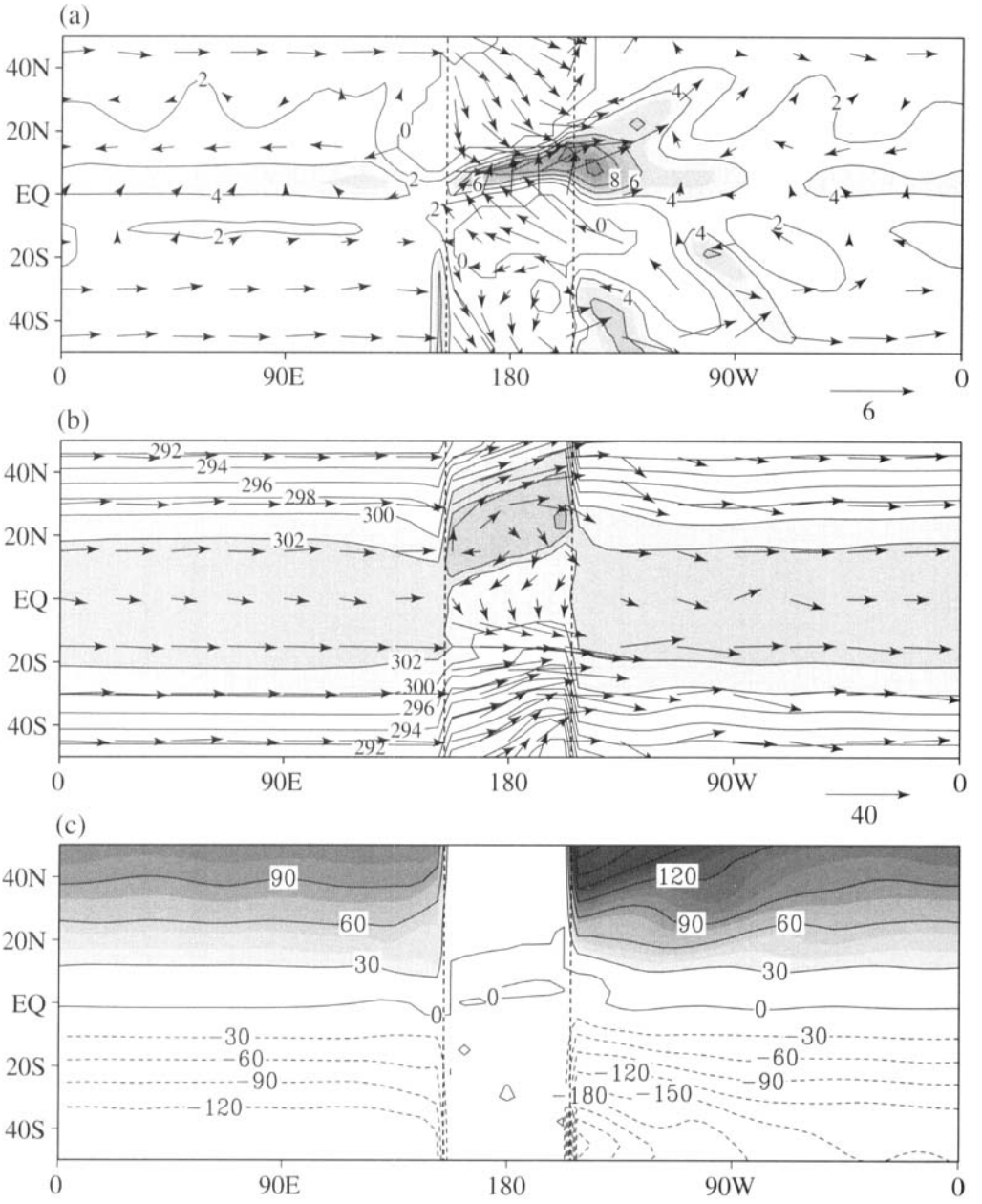

Figure 5. (a) Precipitation (mm day^{-1}) and winds (m s^{-1}) at 850 mb, (b) surface temperature, T_s (K), and wind at 200 mb, and (c) net surface flux into the surface, F_s (W m^{-2}), in June for interactive soil moisture with $Q_{max} = 20$ W m^{-2}. Wind vectors shown at lower density over ocean; scales as given below panel.

varying, can provide such a large-scale factor. Considering non-zero ocean heat transport, Fig. 5(a) shows precipitation for interactive soil moisture with the same Q-flux as Fig. 3. With positive Q-flux in the tropics, the continental region is more favoured for convection than the ocean. Compared with Fig. 4(b), Fig. 5(a) shows not only that continental precipitation is stronger, but also that the maximum precipitation moves further north. For larger ocean transports of heat out of the tropics, the convection zone over

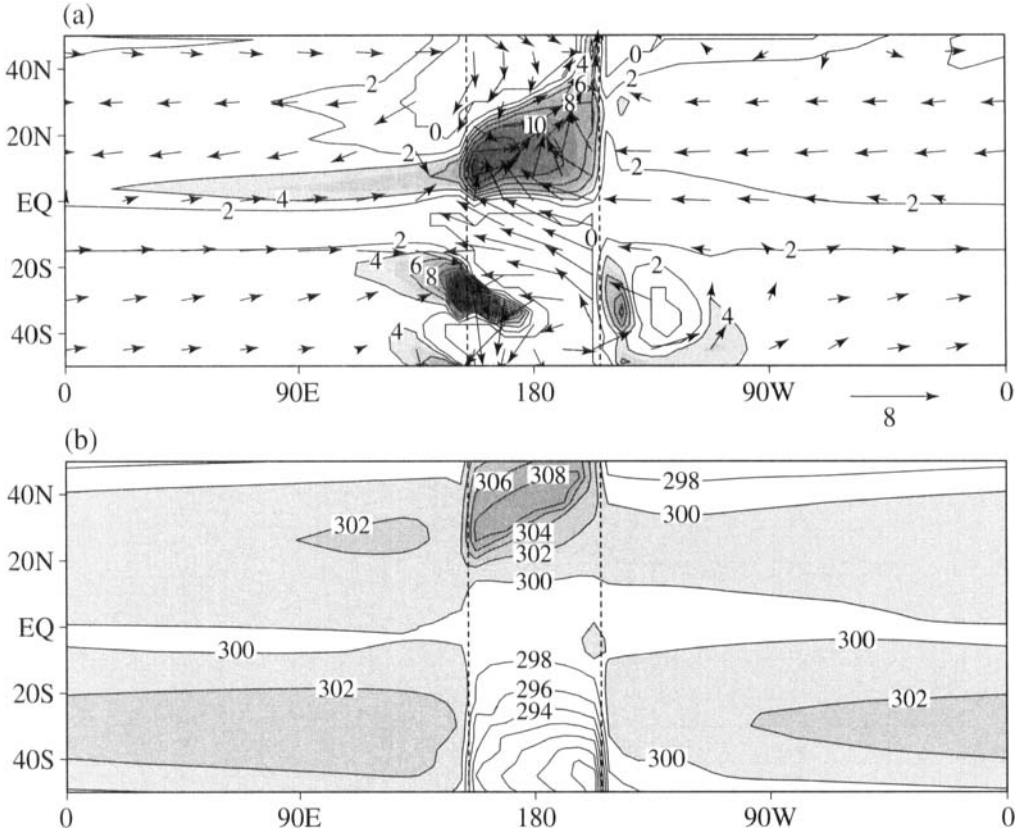

Figure 6. (a) Precipitation (mm day^{-1}) and winds (m s^{-1}) at 850 mb, and (b) surface temperature, T_s (K), in June for interactive soil moisture with $Q_{max} = 50$ W m^{-2}.

the continental region becomes stronger (Fig. 6(a)) and the convection over the ocean becomes weaker. The convergence zone over the continental region moves northward, and it pushes the subsidence region north. The corresponding subtropical circulation imports more moisture from low latitudes for larger Q-flux in the tropics (Fig. 6(a)).

Comparing Fig. 6(b) with Fig. 5(b), the larger Q-flux has the obvious effect of flattening tropical to midlatitude SST gradients. While the 20 W m^{-2} case is a reasonable idealization of observations, the 50 W m^{-2} case serves as an upper bound. The land-surface temperature exhibits a strong seasonal gradient, as expected. Since the summer-hemisphere SST has not warmed as much as the neighbouring continent due to mixed-layer heat capacity, there is a substantial land–ocean contrast, as expected. The land-surface temperature gradient is not a simple function of local thermodynamics, however. It has a spatial dependence within the continent and changes substantially for the experiment with larger Q-flux (Fig. 6(a)). This is partly due to changes in cloud cover and partly to the warmer midlatitude oceans.

A simpler view of the land–ocean constant is provided by the net surface heat flux (Fig. 5(c)). There is a strong net flux into summer-hemisphere oceans balanced by ocean heat storage. Over land, since the heat capacity is low, there is essentially zero net heat flux. Incoming solar flux is returned to the atmosphere by other energy fluxes, providing a relative heating of the atmospheric column compared with neighbouring oceans.

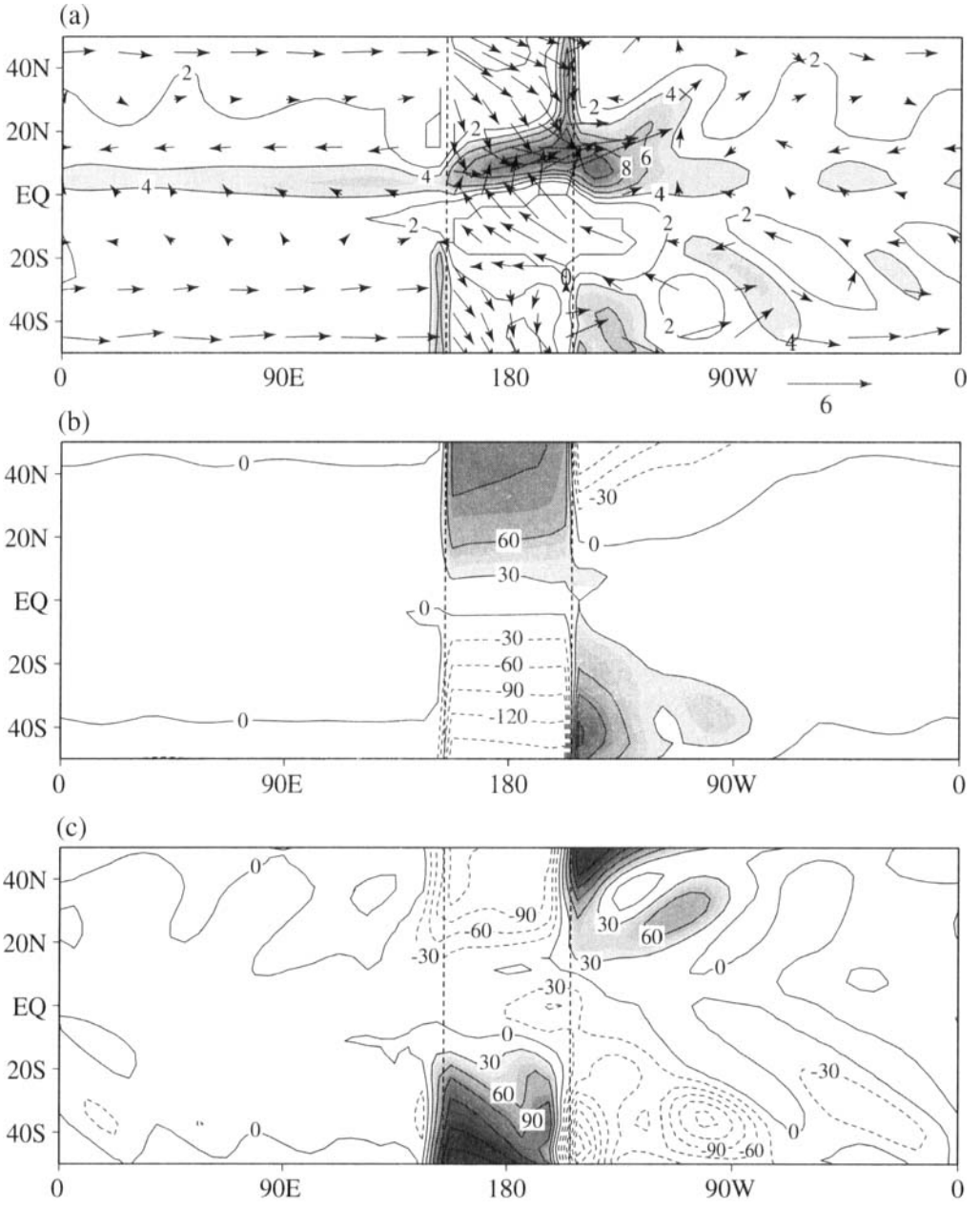

Figure 7. (a) Precipitation (mm day^{-1}) and winds (m s^{-1}) at 850 mb, (b) net flux into the atmosphere, F^{net} (W m^{-2}), and (c) advection of moist static energy, $-\mathbf{v} \cdot \nabla(T + q)$ (W m^{-2}), in June for saturated soil moisture with $Q_{\max} = 20$ W m^{-2}.

(*b*) *Role of 'ventilation' by cross-continental flow*

In the summer hemisphere, the atmosphere over the continent is heated by processes induced by solar radiation, which is the underlying cause for the continental convection zone moving northward. However, the movement of the convection zone does not correspond closely with solar heating. The distribution of the net energy absorbed by the

atmosphere (F^{net}) for an experiment with saturated soil moisture and $Q_{\max} = 20\ \text{W m}^{-2}$ is shown in Fig. 7(b). The maximum F^{net} is much further north than the corresponding precipitation (Fig. 7(a)). With saturated soil moisture, why does the convection zone not move further poleward, as F^{net} would seem to indicate? To understand this, the moist static-energy equation is used

$$\partial_t \langle T + q \rangle + \langle \mathbf{v} \cdot \nabla (T + q) \rangle + \langle \omega \partial_p h \rangle = (g/p_{\text{T}}) F^{\text{net}}, \tag{2}$$

where the moist static energy is $h = s + q$, with s the dry static energy, and $\mathbf{v}$ the horizontal velocity. Temperature, T, and specific humidity, q, are both in energy units with the heat capacity at constant pressure, C_p, and the latent heat per unit mass, L, absorbed. g is gravitational acceleration and ω is pressure velocity. $\langle\ \rangle$ denotes vertical averaging over the troposphere, as defined by

$$\langle X \rangle = p_{\text{T}}^{-1} \int_{p_{\text{t}}}^{p_{\text{s}}} X \, \mathrm{d}p, \tag{3}$$

where p_{s} is surface pressure, p_{t} is pressure at the tropopause and $p_{\text{T}} = p_{\text{s}} - p_{\text{t}}$.

While other mechanisms, such as inertial instability (Tomas and Webster 1997) and a slow precipitation–soil-moisture interaction (Xie and Saiki 1999), could also play a role in determining the location of the convergence zone, this thermodynamic argument is good enough for a first approximation. Considering a steady state and neglecting diffusion, F^{net} is balanced by transports of moist static energy from either convergence (ω term) or advection ($\mathbf{v} \cdot \nabla$ terms). Figure 7(b) shows strong positive F^{net} at midlatitudes. Westerly winds dominate in the column average at midlatitudes. Note that the column average advection differs from advection evaluated at a single level. For instance, easterlies dominate in the subtropics at 850 mb (Fig. 5(a)), but westerlies dominate at 200 mb (Fig. 5(b)). For summer conditions, these westerlies transport relatively cold, low moist static-energy air from the ocean regions into the western part of the continent. This is the pathway by which the continent is impacted by the contrast in net surface flux into the oceans (Fig. 5(c)), with ocean heat storage keeping SST in the summer hemisphere cold. Figure 7(c) shows the distribution of $\mathbf{v} \cdot \nabla (T + q)$ for the experiment in Fig. 7(a). At midlatitudes, the cross-continental flow removes heat over the continent very efficiently. The large-scale environment does not favour convection, so the convection zone does not move as far north as F^{net} would indicate.

For the saturated soil-moisture experiment, $\mathbf{v} \cdot \nabla T$ has the same sign as $\mathbf{v} \cdot \nabla q$ over the continent, because both T and q are higher over the land than over the ocean. For the interactive soil-moisture experiment, the atmosphere over the land is still warmer but is now drier compared with the atmosphere over the ocean. In this case, $\mathbf{v} \cdot \nabla q$ changes sign, but $\mathbf{v} \cdot \nabla T$ becomes more efficient at transporting energy out of the continental areas because lower evaporation induces higher surface temperature. In other words, the ventilation remains strong in the interactive soil-moisture case, but it contributes mainly via the $\mathbf{v} \cdot \nabla T$ term.

To further understand the importance of the ventilation by cross-continental flow, an experiment was conducted with advection effects ($\mathbf{v} \cdot \nabla T$ and $\mathbf{v} \cdot \nabla q$ terms) artificially suppressed. Figure 8(a) shows precipitation for this experiment for a case with interactive soil moisture and with $Q_{\max} = 20\ \text{W m}^{-2}$. The continental convection zone moves substantially further north than the corresponding experiment in Fig. 5(a). Without the ventilation by the cross-continental flow, heating due to the large F^{net} over the continent induces strong convection at the tropics and midlatitudes. The corresponding descent zone is pushed north-westward. Oceans are further disfavoured for convection in general.

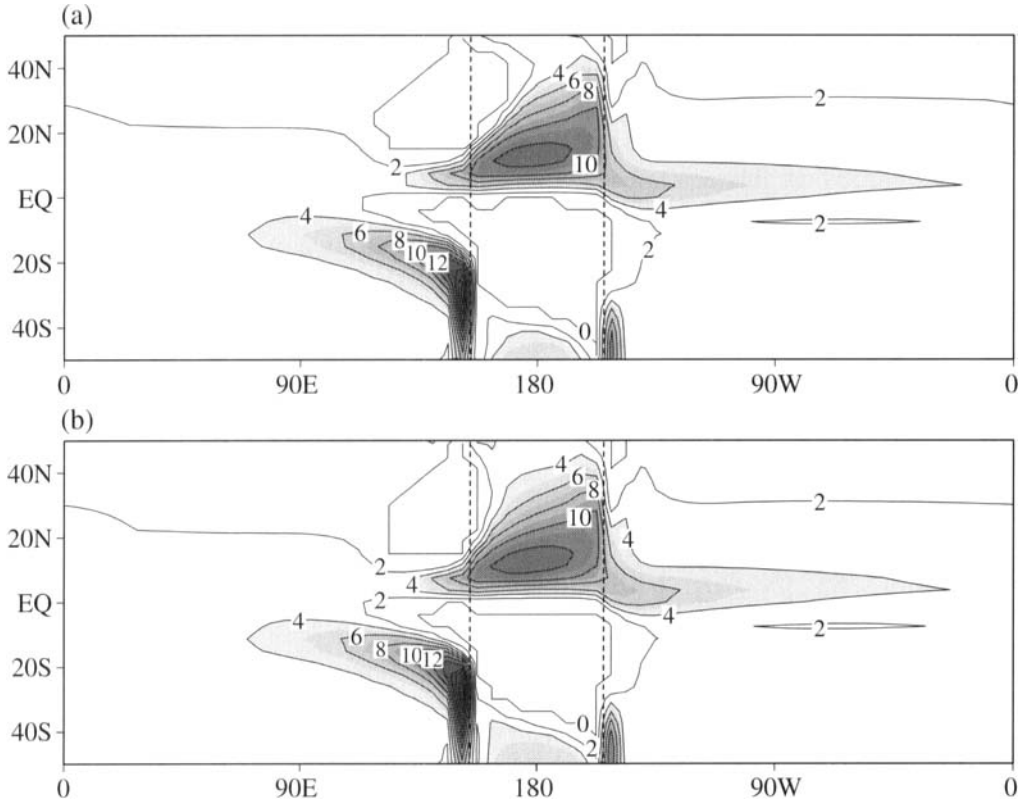

Figure 8. Precipitation (mm day^{-1}) in June for (a) interactive soil moisture and (b) saturated soil moisture with $Q_{max} = 20$ W m^{-2}, in an experiment with advection terms suppressed.

Figure 8(b) shows a similar experiment but with saturated soil moisture. The continental convection zone extends slightly further northward and westward. Overall, however, Figs. 8(a) and (b) resemble each other more than either resembles Figs. 5(a) or 7(a) suggesting that ventilation is more important than the soil-moisture feedback for this case of $Q_{max} = 20$ W m^{-2}. An additional experiment (not shown) for the case of zero ocean transports yields a similar large poleward extent of the convection zone over most of the continent, even with interactive soil moisture. This suggests that the ventilation effect is crucial to the action of the soil-moisture feedback seen in Fig. 4(b). Without cooling by ventilation, the continent, which is heated relative to the surrounding oceans (see Figs. 5(b) and 6(b)), is able to import enough moisture by convergent flow to reverse the soil-moisture feedback. Essentially, if factors in the energy budget strongly favour a convection zone, the soil moisture is secondary.

5. East–West Asymmetry of the Monsoon–Desert Pattern

In the experiments discussed in the previous sections, all have an east–west asymmetry in the pattern of the continental convection zone. The convection zone in the summer continent extends further poleward as one moves east, and the strongest precipitation occurs near the east coast. The desert-like pattern, with little precipitation in the subtropics, extends further south toward the western side of the continent. Qualitatively

similar east–west asymmetries are seen in the observed precipitation patterns in East Asia and South America in the southern summer. The continental configuration makes it harder to compare with North America in this aspect, but it may be noted that the observed precipitation (Xie and Arkin 1996) in the south-eastern USA in July is larger than that in the region associated with the 'Arizona monsoon'.

To examine how this east–west asymmetry arises in the model, we first consider the advection effect $\mathbf{v} \cdot \nabla(T + q)$. At midlatitudes westerly winds dominate, so air with low moist static energy, h, over the ocean replaces the original high-h air over the land as discussed in section 4(b). In the western part of the continent convection decreases, and the atmosphere over that area becomes drier. The north-westerly flow within the continent spreads this effect southward. In the eastern part of the continent, continental-scale flow features further favour convection in this area: wind flow from low latitudes brings high-h air which also contains high moisture. While this latter feature tends to depend also on the convection zone, the westerly flow is largely set by global-scale dynamics. The ventilation by westerlies thus introduces an east–west asymmetry in the thermodynamics on the continental scale.

Another source of the asymmetry is what we term the Rodwell–Hoskins mechanism (Rodwell and Hoskins 1996): a monsoon diabatic heating induces a Rossby wave to the west with associated subsidence. In this study, a strong continental convection occurs along the east coast of the continent. A Rossby-wave pattern induced by this diabatic heating results in subsidence which tends to disfavour convection in this region. A subtropical circulation, induced by the Rossby wave, transports moisture from the tropics and enhances the convection associated with the monsoon diabatic heating in the eastern continent. The subtropical circulation also transports dry air from the midlatitudes and disfavours convection over the western continent. This further enhances the asymmetry in the continental convection-zone pattern. This circulation-induced feedback to the asymmetry has also been discussed by Xie and Saiki (1999). Because the convection itself interacts with the circulation associated with the compensating Rossby-wave descent, we refer to the entire process as the 'interactive Rodwell–Hoskins mechanism'.

We wish to determine the relative importance of ventilation versus the interactive Rodwell–Hoskins mechanism in creating the east–west asymmetry in the convection. The effect of the cross-continental flow on the east–west asymmetry can be inferred from the experiments, with advection turned off, that are discussed in section 4(b) and shown in Fig. 8. Without advection, the precipitation over the continent moves further northward, but some east–west asymmetry persists, even with saturated soil moisture (Fig. 8(b)). Suppressing the ventilation has such a large impact on the shape of the continental convection zone that it is difficult to say whether the asymmetry is larger or smaller. Without advection the descent zone is confined to the western part of the continent, while both the interior and the eastern continent tend to be convecting.

To further examine the interactive Rodwell–Hoskins mechanism, a fixed f is used over the northern hemisphere to eliminate the β-effect and thus the Rossby-wave propagation. Specifically the value of f from 13.125°N is applied to all latitudes north of 1.875°N. Advection is suppressed ($\mathbf{v} \cdot \nabla T = 0$ and $\mathbf{v} \cdot \nabla q = 0$) as in the previous experiment. Figure 9(a) shows precipitation without effects of the horizontal advection and the Rossby wave. The east–west asymmetry disappears. The only difference between Fig. 8(a) and Fig. 9(a) is the β-effect. This implies that the Rossby-wave dynamics associated with the β-effect also contribute to the east–west asymmetry, in addition to the effect of the cross-continental flow.

Comparing F^{net} in Fig. 9(b) with the precipitation in Fig. 9(a), the location of the precipitation is consistent with what F^{net} indicates. The continental convection

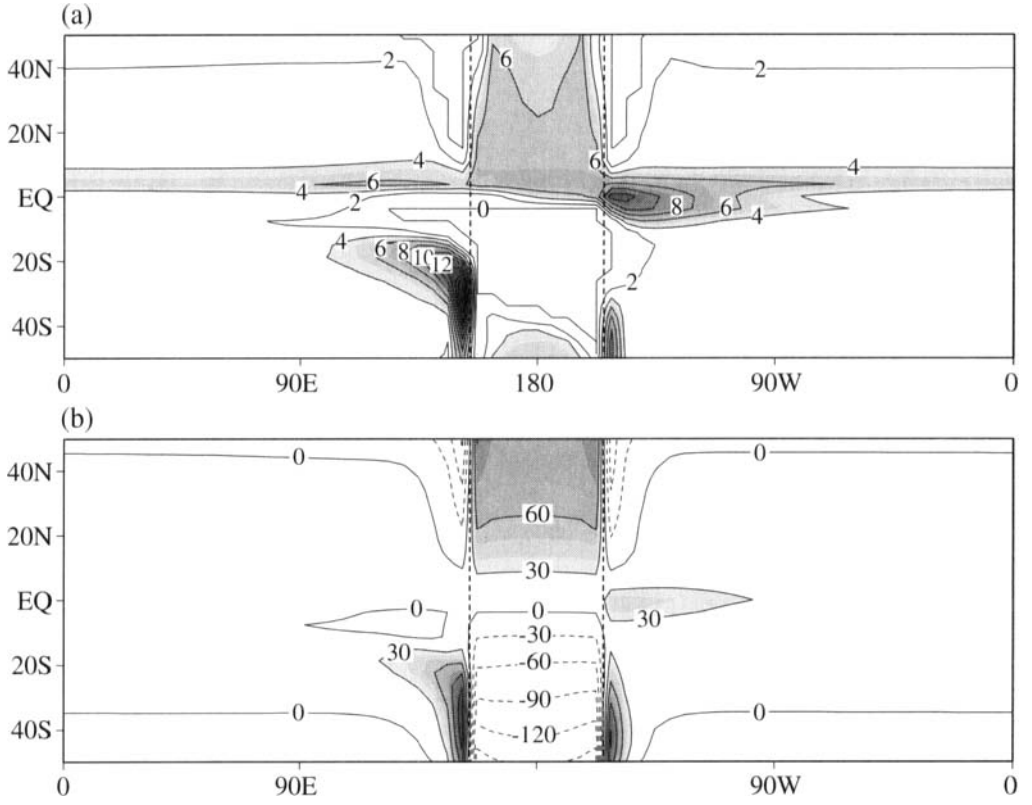

Figure 9. (a) Precipitation (mm day^{-1}) and (b) net flux into the atmosphere, F^{net} (W m^{-2}), in June for interactive soil moisture with $Q_{max} = 20$ W m^{-2} in an experiment with the Coriolis parameter, f, set to a constant in the northern hemisphere, and advection terms suppressed.

zone moves further north than previously conducted experiments. Without the cross-continental flow effect and the β-effect, the continental convection occurs where atmospheric heating by fluxes into the column occurs. Contrasting this case with the control (Fig. 5), both the ventilation and Rossby-wave mechanism prevent the continental convection zone from moving northward.

Ideally we also want to do an experiment with the β-effect but no ventilation. This experiment is hard to design because β affects midlatitude winds which also change the ventilation effect. Inferring from the difference between the case with no ventilation (Fig. 8) and the case with ventilation (Fig. 7), as well as the case with no ventilation (Fig. 8) and the case with no ventilation and no β-effect (Fig. 9), we conclude that ventilation is more important than the β-effect, although both contribute to the asymmetry in the land precipitation pattern.

6. WIDER-CONTINENT CASES

For all experiments in the previous sections, a continent of width (45° in longitude) that is similar to Africa or South America is used. If the continent becomes wider, similar to Eurasia, one might expect some changes in the previous results. For instance, the ventilation effect might be less important in limiting the northward movement of the continental convection zone. We thus examine the impact of the width of a continent on

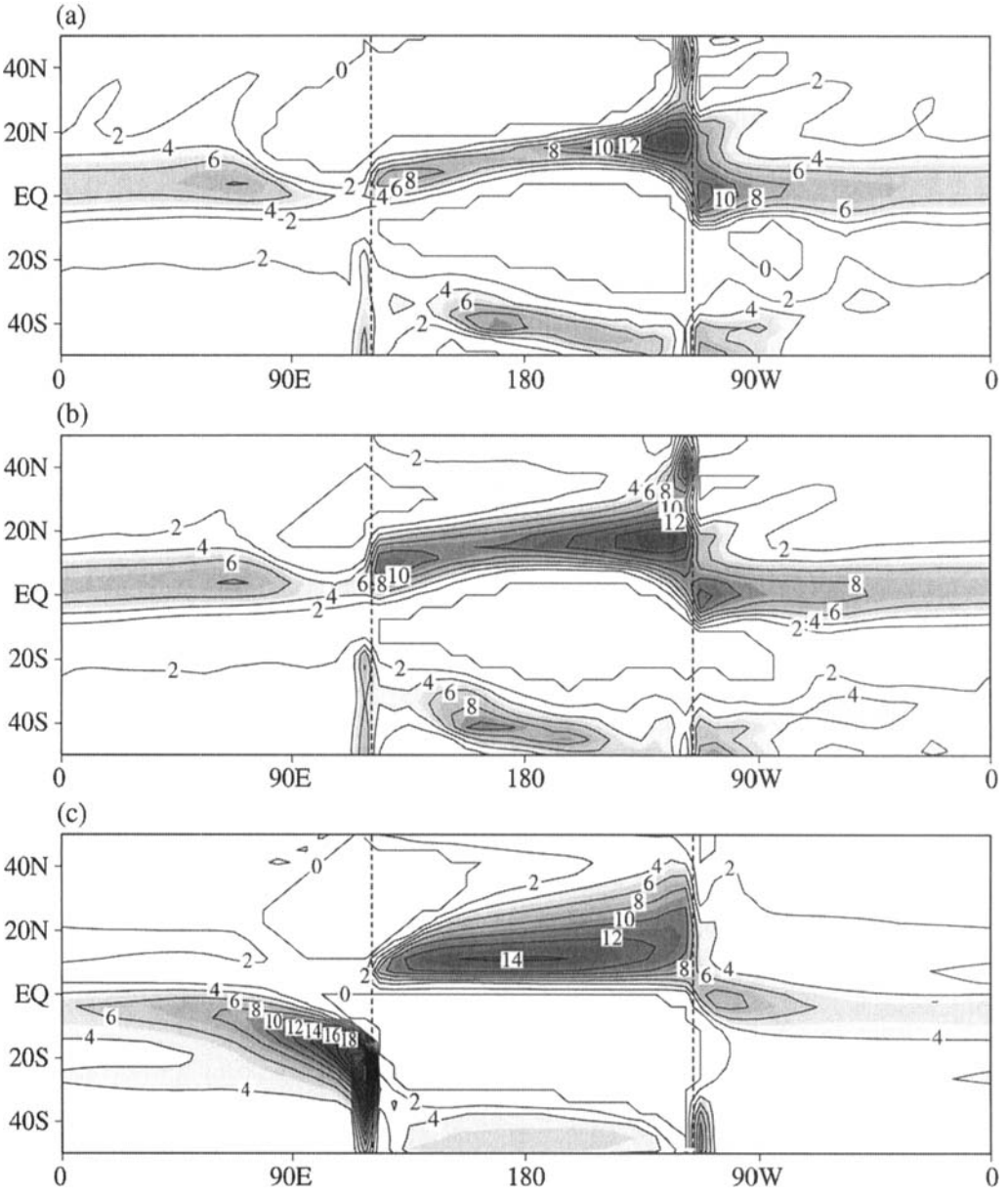

Figure 10. Precipitation (mm day^{-1}) in June for experiments with a wider continent, $Q_{max} = 20$ W m^{-2}, (a) interactive soil moisture (with advection terms), (b) saturated soil moisture (with advection terms), or (c) interactive soil moisture and advection terms suppressed.

the continental convection. In an experiment with a wider continent (120° in longitude), interactive soil moisture and $Q_{max} = 20$ W m^{-2}, the precipitation pattern over the continent (Fig. 10(a)) is similar to the precipitation pattern in the control run (Fig. 5(a)). The continental convection zone in Fig. 10(a) is stretched out and extended over the whole continent in the east–west direction. The north-east–south-west tilting of the convection zone is still seen in Fig. 10(a). Although the angle of the north-east–south-west tilt of the convection zone is smaller than in the control case (12° versus 8°), the

convection zone still extends further north on the eastern side in the wider-continent case. While the centre of the continental convection zone is located around 10°N in the eastern continent for the control run (Fig. 5(a)), the convection zone in Fig. 10(a) is around 20°N on the east side of the continent. There is a strong, narrow extension of the convection zone up the eastern coast (although the intensity of this feature might be overestimated by this model; see ZNC). For the case with saturated soil moisture (Fig. 10(b)), the continental convection zone is quite similar to the interactive soil-moisture case, except the convection extends slightly further north. This is similar to the corresponding comparison between Fig. 5(a) and Fig. 7(a), but with the convection zone stretched over the wider continent.

The result in Fig. 10(a) suggests that the ventilation caused by the westerlies is still a dominant effect because the northward movement of the continental convection zone is still relatively further south than the corresponding F^{net} indicates. To confirm the importance of the ventilation effect, we suppress the horizontal advection terms (i.e. both $\mathbf{v} \cdot \nabla T$ and $\mathbf{v} \cdot \nabla q$ are zero). The continental convection zone for this experiment (Fig. 10(c)) moves considerably further northward compared with Fig. 10(a). Thus the ventilation is still of leading importance in limiting the northward movement of the continental convection zone even with a wider continent. The east–west asymmetry of the continental convection zone is also found in this wider-continent experiment. The similarity between Fig. 8(a) and Fig. 10(c) indicates the importance of the ventilation effect on the east–west asymmetry of the continental convection zone, as well as the effect of the interactive Rodwell–Hoskins mechanism.

7. SUMMARY AND CONCLUSIONS

The monsoon has great differences in detail in different regions, but at its heart is the seasonal movement of land convection zones, studied here on an idealized rectangular continent. An intermediate atmosphere–land model coupled to a simple mixed-layer model ocean is used to analyse the sources of land–ocean contrast, which include ocean transports, ocean mixed-layer heat capacity and soil moisture. Experiments are performed to compare the importance of these and to isolate the mechanisms of ocean–atmosphere–land interaction by which these affect continental convection zones.

First, assuming the sun in the equinox, effects of soil moisture and ocean heat transport are examined. A case with no ocean transports (zero Q-flux) permits a view of the effect of soil moisture on monsoon precipitation. We compare the results of two experiments: saturated soil moisture and interactive soil moisture. At midlatitudes, the descending branch of the Hadley cell occurs over both land and ocean. Because of this large-scale descent, convection is not favoured for this area. With interactive land hydrology, land evaporation decreases compared with ocean evaporation as soil moisture drops. Sensible heat becomes dominant in the balance of surface heat fluxes. CAPE over the land is less, so convection over land decreases as well. Less precipitation makes the land drier and favourable to desertification. When soil moisture is forced to be saturated, evaporation over the land is as efficient as over the ocean, so precipitation is similar over land and over ocean. Figure 11(a) summarizes these soil-moisture effects schematically, focusing on the northern hemisphere. Qualitatively similar effects in northern summer are discussed below.

To understand the first-order effects of ocean transport, a Q-flux distribution varying only with latitude is used. Figure 11(b) explains how the ocean transport can affect the monsoon. This is seen in the simplest form in the equinox case, but extends also to the summer-monsoon case. When the ocean transports heat out of the tropics and the

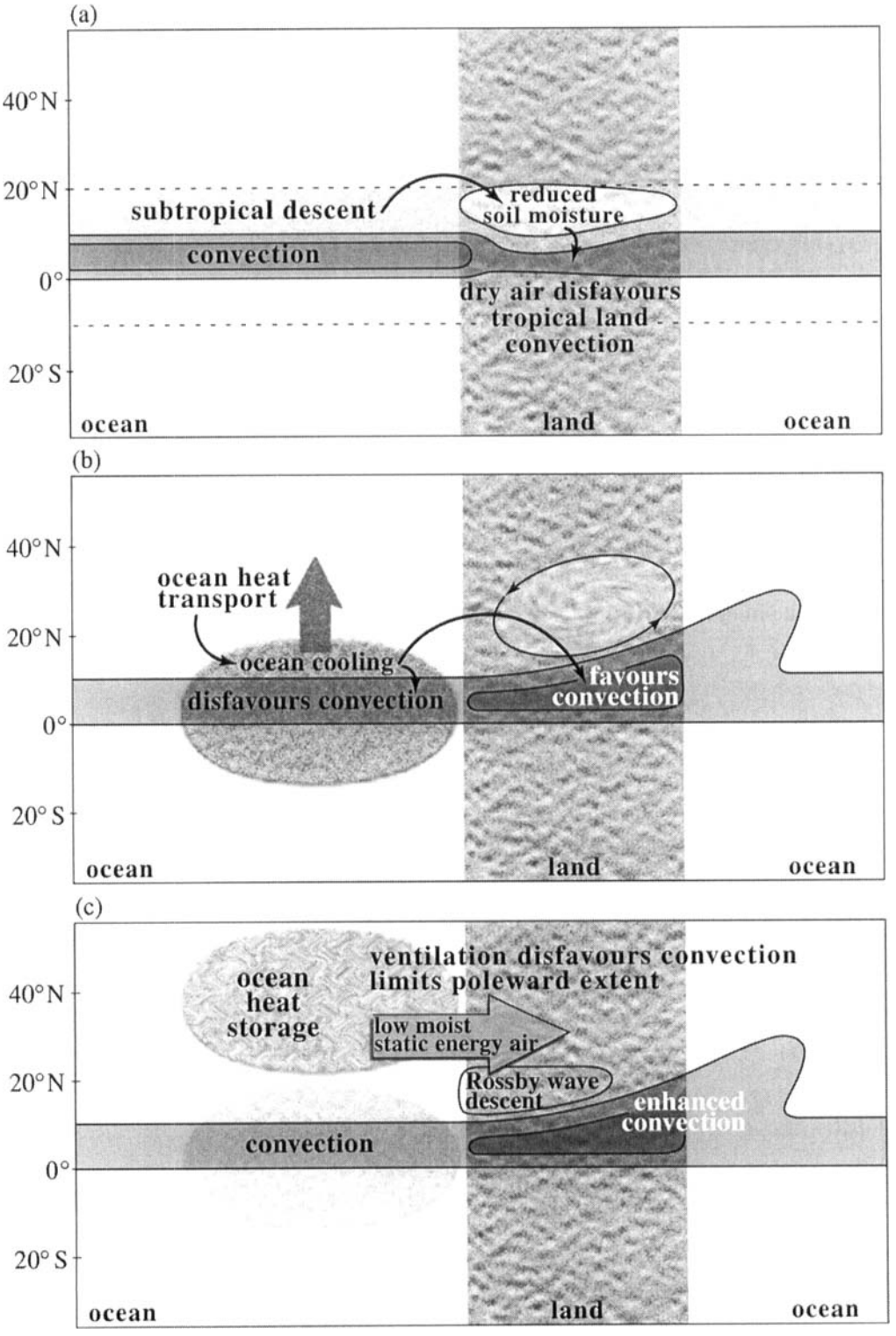

Figure 11. Schematic diagrams describing effects on continental convection zones (for northern-hemisphere summer) of (a) soil-moisture feedbacks, (b) ocean heat transport out of the tropics, and (c) ventilation and the interactive Rodwell–Hoskins mechanism.

subtropics, the tropical land becomes a relative heat source in terms of net flux into the atmospheric column (positive and greater F^{net}). This relative heat source favours convection and establishes a continental convection zone (strong land precipitation). In the equinox case, because of the increase in land precipitation and the decrease in ocean precipitation in the tropics, the Hadley cell over the land becomes stronger, while the Hadley cell over the ocean weakens. Because the convergent circulation flowing into the higher-F^{net} region carries sufficient moisture supply, this occurs whether soil moisture is saturated or unsaturated.

This competition between the soil-moisture feedback (tending to disfavour continental regions) and ocean heat transport (tending to favour tropical continental regions) continues as we turn to examine the seasonal variation of the continental convection zones. However, other factors also become important, as summarized in Table 1. During the northern summer, the maximum heating of the atmosphere over the land moves northward because of the maximum solar insolation and smaller heat capacity of the land. Despite the northward maximum of solar insolation, the continental convection zone does not move northward even when the soil moisture is saturated and positive Q-flux is used (ocean heat flux out of the tropics). In our analysis, ventilation by the cross-continental flow plays a very important role in limiting the northward movement of the continental convection zone (see Fig. 11(c)). At midlatitudes, dominant westerly winds blow colder air with low moist static energy from the ocean and replace the original warm air with high moist static energy over the land. This ventilation is very effective at opposing the warming tendency due to the large insolation and prevents conditions thermodynamically favourable to deep convection from occurring over continental subtropical and midlatitude regions. Together with the subsidence of the Hadley cell, it also creates favourable conditions for desertification over parts of the subtropical land. When Q-flux is increased in the tropics, the increased contrast with ocean regions favours land convection and the monsoon circulation becomes stronger. If the monsoon circulation becomes strong enough, ventilation will be controlled by the monsoon circulation not by the westerly winds. The monsoon circulation transports warm and moist air from the tropics, so the continental monsoon precipitation increases and the convergence zone of the monsoon moves northward. We note that even annually averaged ocean heat transports have an important effect on the seasonal monsoon precipitation.

In all experiments in this study, continental monsoon precipitation with seasonal variation has a clear east–west asymmetry. There are two possible explanations: the interactive Rodwell–Hoskins mechanism and the ventilation by cross-continental flow. The Rodwell–Hoskins mechanism provides subsidence induced by monsoon diabatic heating in the east to create desert-like conditions in the west (the term 'interactive Rodwell–Hoskins mechanism' emphasizes that this, in turn, interacts with the convective heating). The ventilation effect introduces asymmetry because the winds blow preferentially from east or west (depending on the latitude). For instance, midlatitude westerly winds advect air with low moist static energy from the neighbouring ocean into the western part of the continent (where it is redistributed by the monsoon circulation) aiding production of deserts in the west. The monsoon circulation, with cyclonic circulation in the lower troposphere, transports moisture from low latitudes to the eastern part of the land. Without the ventilation associated with horizontal advection, the convection zone over the land would move further north (Figs. 8(a) and (b)). Because the Rodwell–Hoskins mechanism depends on Rossby-wave dynamics, one way of testing its impact is to perform experiments that suppress the β-effect. The experiments in Fig. 8 and Fig. 9 show that the interactive Rodwell–Hoskins mechanism and ventilation each produce an inherent east–west asymmetric pattern of land precipitation (see Fig. 11(c)). Overall, it

TABLE 1. PROCESSES AFFECTING CONTINENTAL CONVECTION ZONES

Processes		Effects
Soil moisture	•	drying tendency in subtropical descent region (from previous seasons)
	⇒	contributes to limiting poleward extension of convection over land
	⇒	tropical continent convection disfavoured (relative to tropical ocean)
Ocean heat transport	•	tropical ocean cooled by transport
	⇒	tropical continent convection favoured
Ventilation	•	import of low moist static-energy air from ocean where heat storage opposes summer warming
	⇒	midlatitude continent not thermodynamically favoured
	⇒	limits poleward extension of summer monsoon convection over land
	⇒	western continent disfavoured (relative to eastern continent)
Interactive Rodwell–Hoskins mechanism	•	Rossby-wave divergence/convergence pattern interacts with convection
	⇒	eastern continent convection favoured
	⇒	western continent convection disfavoured

Bullets denote the description of the process; arrows indicate the effects on continental convection.

appears that the ventilation effect is the dominant of the two. We underline a caveat on these experiments using drastic changes, such as fixed f. Care must be used in using such idealized experiments to interpret monsoon dynamics in realistic situations.

In the real world, seasonal movements and locations of continental convection zones are affected by additional factors such as topography, continental shape and zonal SST gradients (Hahn and Manabe 1975; Stone and Chervin 1984). The width of the continent appears to be a secondary factor (for widths in the range 45° to 120° longitude). The simplified experiments presented here already exhibit complex oppositions among several processes, listed in Table 1. Most of this complexity is associated with moving from the context of fixed SST experiments to a system in which the sources of land–sea contrast are more explicitly examined. For instance, although ocean transports are represented very simply here, the results suggest that their role in transporting heat out of tropical oceans is very important to the continental convection zones, creating contrast between tropical ocean and land regions that favours land convection. The role of ocean heat transports includes an impact on seasonal migration of the land monsoon, even if the ocean transport does not itself vary with season.

Of the processes in Table 1, the ventilation effect appears to be of leading importance in limiting the poleward progression of the convection zone as the region of maximum insolation moves poleward in summer. Soil-moisture feedbacks play an additional role once the leading effect of ventilation is taken into account. Likewise, the Rossby-wave dynamics of the interactive Rodwell–Hoskins mechanism can add to the east–west asymmetry of the continental monsoon and descent regions, but much of this asymmetry has already been introduced by the ventilation.

ACKNOWLEDGEMENTS

This work was supported under National Science Foundation grant ATM-0082529, National Oceanic and Atmospheric Administration grant NA86GP0314, Pan-American Climate System grant NA86GP0361 and National Aeronautics and Space Administration grant NA G5-9358. This is the University of California, Los Angeles, Institute

of Geophysics and Planetary Physics contribution 5463. The authors thank B. Hoskins, J. McWilliams and M. Yanai for discussions, J. E. Meyerson for graphics and T. Rippeon for proof reading. It is a pleasure to acknowledge N. Zeng for much joint work on model development, and for creation of the land-surface model.

REFERENCES

Betts, A. K. and Miller, M. J. 1986 A new convective adjustment scheme. Part II: Single column tests using GATE wave, BOMEX, ATEX and arctic air-mass data sets. *Q. J. R. Meteorol. Soc.*, **112,** 693–709

1993 The Betts–Miller scheme. Pp. 107–121 in *The representation of cumulus convection in numerical models of the atmosphere.* Eds. K. A. Emanuel and D. J. Raymond. Meteorol. Monog. **24** No. 46. Am. Meteorol. Soc.

Chou, C. 1997 'Simplified radiation and convection treatments for large-scale tropical atmospheric modeling'. PhD dissertation, University of California

Chou, C. and Neelin, J. D. 1996 Linearization of a longwave radiation scheme for intermediate tropical atmospheric models. *J. Geophys. Res.*, **101,** 15129–15145

1999 Cirrus detrainment-temperature feedback. *Geophys. Res. Lett.*, **26,** 1295–1298

2001 Mechanisms limiting the southward extent of the South American summer monsoon. *Geophys. Res. Lett.*, in press

Cook, K. H. and Gnanadesikan, A. 1991 Effects of saturated and dry land surfaces on the tropical circulation and precipitation in a general circulation model. *J. Climate,* **4,** 873–889

Dirmeyer, P. A. 1998 Land–sea geometry and its effect on monsoon circulations. *J. Geophys. Res.*, **103,** 11555–11572

Doney, S. C., Large, W. G. and Bryan, F. O. 1998 Surface ocean fluxes and water-mass transformation rates in the coupled NCAR climate system model. *J. Climate,* **11,** 1420–1441

Flohn, H. 1957 Large-scale aspects of the 'summer monsoon' in south and east Asia. *J. Meteorol. Soc. Jpn.*, **35,** 180–186

Fu, Q. and Liou, K. N. 1993 Parameterization of the radiative properties of cirrus clouds. *J. Atmos. Sci.*, **50,** 2008–2025

Hahn, F. G. and Manabe, S. 1975 The role of mountains in the South Asian monsoon. *J. Atmos. Sci.*, **32,** 1515–1541

Hansen, J., Fung, I., Lacis, A., Rind, D., Lenedeff, S., Ruedy, R. and Russell, G. 1988 Global climate changes as forecast by the Goddard Institute for Space Studies three-dimensional model. *J. Geophys. Res.*, **93D,** 9341–9364

Hansen, J., Ruedy, R., Lacis, A., Russell, G., Sato, M., Lerner, J., Rind, D. and Stone, P. 1997 Wonderland climate model. *J. Geophys. Res.*, **102,** 6823–6830

Ju, J. and Slingo, J. M. 1995 The Asian summer monsoon and ENSO. *Q. J. R. Meteorol. Soc.*, **122,** 1133–1168

Keith, D. W. 1995 Meridional energy transport: Uncertainty in zonal means. *Tellus*, **47A,** 30–44

Latif, M., Sterl, A., Assenbaum, M., Junge, M. M. and Maier-Reimer, E. 1994 Climate variability in a coupled GCM. Part II: The Indian Ocean and monsoon. *J. Climate,* **7,** 1449–1462

Lofgren, B. M. 1995 Surface albedo–climate feedback simulated using two-way coupling. *J. Climate,* **8,** 2543–2562

Meehl, G. A. 1989 The coupled ocean–atmosphere modeling problem in the tropical Pacific and Asian monsoon region. *J. Climate,* **2,** 1146–1163

1994 Influence of the land surface in the Asian summer monsoon: External conditions versus internal feedbacks. *J. Climate,* **7,** 1033–1049

Miller, J. R., Russell, G. L. and Tsang, L.-C. 1983 Annual oceanic heat transports computed from an atmospheric model. *Dyn. Atmos. Oceans*, **7,** 95–109

Murakami, T. 1987 Orography and monsoons. Pp. 331–364 in *Monsoons.* Eds. J. S. Fein and P. L. Stephens. John Wiley, New York, USA

Neelin, J. D.	1997	Implications of convective quasi-equilibrium for the large-scale flow. Pp. 413–446 in *The physics and parameterization of moist atmospheric convection.* Ed. R. K. Smith. Kluwer Academic Publishers, Dordrecht, the Netherlands
Neelin, J. D. and Yu, J.-Y.	1994	Modes of tropical variability under convective adjustment and the Madden–Julian Oscillation. Part I: Analytical theory. *J. Atmos. Sci.*, **51,** 1876–1894
Neelin, J. D. and Zeng, N.	2000	The quasi-equilibrium tropical circulation model—formulation. *J. Atmos. Sci.*, **57,** 1741–1766
Nobre, P. and Shukla, J.	1996	Variations of sea surface temperature, wind stress and rainfall over the tropical Atlantic and South America. *J. Climate,* **9,** 2464–2479
Rodwell, M. J. and Hoskins, B. J.	1996	Monsoons and the dynamics of deserts. *Q. J. R. Meteorol. Soc.*, **122,** 1385–1404
Russell, G. L., Miller, J. R. and Tsang, L.-C.	1985	Seasonal oceanic heat transports computed from an atmospheric model. *Dyn. Atmos. Oceans*, **9,** 253–271
Sellers, P. J., Mintz, Y., Sud, Y. C. and Dalcher, A.	1986	A simple biosphere model (SiB) for use within general circulation models. *J. Atmos. Sci.*, **43,** 505–531
Shen, S. and Lau, K. M.	1995	Biennial oscillation associated with the east Asian monsoon and tropical sea surface temperatures. *J. Meteorol. Soc. Jpn.*, **73,** 105–124
Shukla, J. and Fennessy, M. J.	1994	'Simulation and predictability of monsoons'. In Proceedings of the International conference on monsoon variability and prediction. Tech. Rep. WCRP-84, World Climate Research Programme, Geneva, Switzerland
Sperber, K. R. and Palmer, T. N.	1996	Interannual tropical rainfall variability in general circulation model simulations associated with the atmospheric model intercomparison project. *J. Climate,* **9,** 2727–2750
Srinivasan, J., Gadgil, S. and Webster, P. J.	1993	Meridional propagation of large-scale monsoon convective zones. *Meteorol. Atmos. Phys.*, **52,** 15–35
Stone, P. H. and Chervin, R. M.	1984	The influence of ocean surface temperature gradient and continentality on the Walker circulation. Part II: Prescribed global changes. *Mon. Weather Rev.,* **112,** 1524–1534
Tian, S. F. and Yasunari, T.	1992	Time and space structure of interannual variations in summer rainfall over China. *J. Meteorol. Soc. Jpn.,* **70,** 585–596
Tomas, R. A. and Webster, P. J.	1997	The role of inertial instability in determining the location and strength of near-equatorial convection. *Q. J. R. Meteorol. Soc.,* **123,** 1445–1482
Trenberth, K. E., Branstator, G. W., Karoly, D., Kumar, A., Lau, N.-C. and Ropelewski, C.	1998	Progress during TOGA in understanding and modeling global teleconnections associated with tropical sea surface temperatures. *J. Geophys. Res.,* **103,** 14291–14324
Webster, P. J.	1987	The elementary monsoon. Pp. 3–32 in *Monsoons.* Eds. J. S. Fein and P. L. Stephens. John Wiley, New York, USA
	1994	The role of hydrological processes in ocean–atmosphere interactions. *Rev. of Geophys.*, **32,** 427–476
Webster, P. J. and Chou, L.	1980a	Seasonal structure of a simple monsoon structure. *J. Atmos. Sci.*, **37,** 354–367
	1980b	Low frequency transitions of a simple monsoon system. *J. Atmos. Sci.*, **37,** 368–382
Webster, P. J. and Yang, S.	1992	Monsoon and ENSO: Selectively interactive systems. *Q. J. R. Meteorol. Soc.,* **118,** 877–926
Webster, P. J., Magaña, V. O., Palmer, T. N., Shukla, J., Tomas, R. A., Yanai, M. and Yasunari, T.	1998	Monsoons: Processes, predictability, and the prospects for prediction. *J. Geophys. Res.,* **103,** 14451–14510
Xie, P. and Arkin, A.	1996	Analyses of global monthly precipitation using gauge observations, satellite estimates, and numerical model predictions. *J. Climate,* **9,** 840–858
Xie, S.-P. and Saiki, N.	1999	Abrupt onset and slow seasonal evolution of summer monsoon in an idealized GCM simulation. *J. Meteorol. Soc. Jpn.,* **77,** 949–968
Xue, Y. and Shukla, J.	1993	The influence of land surface properties on Sahel climate. Part I: Desertification. *J. Climate*, **5,** 2232–2245
Yanai, M., Li, C. and Song, Z.	1992	Seasonal heating of the Tibetan Plateau and its effects on the evolution of the Asian summer monsoon. *J. Meteorol. Soc. Jpn.,* **70,** 319–351

Yanai, M. and Li, C. 1994 Mechanism of heating and the boundary layer over the Tibetan Plateau. *Mon. Weather Rev.,* **122,** 305–323

Yang, S. and Lau, K.-M. 1998 Influences of sea surface temperature and ground wetness on Asian summer monsoon. *J. Climate,* **11,** 3230–3246

Young, J. A. 1987 Physics of monsoons: The current view. Pp. 211–243 in *Monsoons*. Eds. J. S. Fein and P. L. Stephens. John Wiley, New York, USA

Yu, J.-Y. and Neelin, J. D. 1994 Modes of tropical variability under convective adjustment and the Madden–Julian Oscillation. Part II: Numerical results. *J. Atmos. Sci.,* **51,** 1895–1914

Zeng, N., Neelin, J. D. and Chou, C. 2000 The first quasi-equilibrium tropical circulation model—implementation and simulation. *J. Atmos. Sci.,* **57,** 1767–1796